Available online at www.sciencedirect.com

SciVerse ScienceDirect

Solar Energy 88 (2013) 137–143

SOLAR ENERGY

www.elsevier.com/locate/solener

Tuning photocurrent response through size control of CdTe quantum dots sensitized solar cells

Ali Badawi [a,b], N. Al-Hosiny [b], Said Abdallah [b,c,*], S. Negm [c], H. Talaat [a]

[a] Physics Department, Faculty of Science, Ain Shams University, Abbassia, Cairo, Egypt
[b] Department of Physics, Faculty of Science, Taif University, Taif, Saudi Arabia
[c] Department of Mathematical and Physical Engineering, Faculty of Engineering (Shoubra), Benha University, Cairo, Egypt

Received 28 July 2012; received in revised form 4 November 2012; accepted 7 November 2012
Available online 23 December 2012

Communicated by: Associate Editor Takhir Razykov

Abstract

The photovoltaic performance of CdTe quantum dots (QDs) sensitized solar cells (QDSSCs) as a function of tuning the band gap of CdTe QDs size is studied. The tuning of band gap was carried out through controlling the size of QDs. Presynthesized CdTe QDs of radii from 2.1 nm to 2.5 nm) were deposited by direct adsorption (DA) technique onto a layer of TiO_2 nanoparticles (NPs) to serve as sensitizers for the solar cells. The characteristic parameters of the assembled QDSSCs were measured under AM 1.5 sun illuminations. The values of current density (J_{sc}) and overall efficiency (η) increase with decreasing CdTe QDs size, since the lowest unoccupied molecular orbital (LUMO) levels shifts closer to vacuum level, which causes an increase in the driving force. Consequently the electrons' injections to the conduction band (CB) of TiO_2 NPs become faster. The maximum values of J_{sc} (1105 μA/cm^2) and η (0.190%) were obtained for the smallest CdTe QDs size (2.10 nm). The open circuit voltages (V_{oc}) varies slightly with the size of the CdTe QDs, however it is only dictated by the CB level of TiO_2 NPs and the VB of the electrolyte. Furthermore, the photocurrent response of the assembled cells to ON–OFF cycles of the illumination indicates the prompt generation of anodic current.

Keyword: CdTe quantum dots sensitized solar cells; Tuning photocurrent response; Photovoltaic

1. Introduction

In recent years, there has been a concerted effort to enhance the performance of quantum dot sensitized solar cells (QDSSCs) (Tvrdy et al., 2011; Zhou et al., 2012; Zhao et al., 2012; Xie et al., 2012; Yu et al., 2011). Semiconductor quantum dots (QDs) exhibit attractive characteristics as sensitizers due to their tunable band gaps through size control, that could be used to match the solar spectrum (Xie et al., 2012; Kamat, 2007; Bang and Kamat, 2009; Tubtimtae et al., 2010; Timp and Zhu, 2010; Li et al., 2011; Giḿenez et al., 2009; Fan et al., 2009; Lin and Lee, 2011; Tvrdy and Kamat, 2009; Wu, 2004; McCandless and Dobson, 2004). In addition, QDs possess higher extinction coefficients (Xie et al., 2012; Tubtimtae et al., 2010; Lin and Lee, 2011; Kim et al., 2011; Yang and Chang, 2010), higher stability (Li et al., 2011; Yum et al., 2007) (as compared to metal–organic dyes), and a large intrinsic dipole moment leading to rapid charge separation (Giḿenez et al., 2009; Prabakar et al., 2009; Emin et al., 2011; Smith et al., 2008), and intrinsically strong absorption (Tubtimtae et al., 2010). Furthermore, QDs have been shown recently to produce highly efficient multiple exciton generation (MEG) (Xie et al., 2012; Tubtimtae et al., 2011; Nozik, 2008), whereby a single absorbed photon can generate

* Corresponding author at: Department of Physics, Faculty of Science, Taif University, Taif, Saudi Arabia. Tel.: +966 553680201; fax: +966 27241880.
E-mail address: dr.saiedabdallah@yahoo.com (Said Abdallah).

0038-092X/$ - see front matter © 2012 Elsevier Ltd. All rights reserved.
http://dx.doi.org/10.1016/j.solener.2012.11.005

more than one electron–hole pair (Tubtimtae et al., 2010; Fan et al., 2009; Nozik, 2008; Yu et al., 2006). Many studies were carried out on photovoltaic cells using QDs such as CdSe (Wijayanthaa et al., 2004), CdS (Bang and Kamat, 2009; Guijarro and Lana-Villarreal, 2009), CdTe (Bang and Kamat, 2009; Kniprath et al., 2009; Yong Kim et al., 2004; Wang et al., 2010), PbS (Hyun et al., 2008), PbSe (Kitada et al., 2009), InAs (Yu et al., 2006), $Cu_{2-x}S$ (Lin and Lee, 2011), Ag_2Se (Tubtimtae et al., 2011), and Ag_2S (Xie et al., 2012; Tubtimtae et al., 2010) for harvesting solar radiation in the visible and infrared regions. In the case of QDSSCs, excited electrons of semiconductor nanocrystals are injected into a large band gap semiconductor such as TiO_2 or ZnO, while holes are scavenged by a redox couple. By controlling the size of these semiconductor QDs, one can readily tune the band energies as well as the photoresponse of the solar cell. Since QDSSCs have large surface areas, they would provide a technically and economically credible alternative to conventional cells; silicon photovoltaic or dye-sensitized solar cells (DSSCs). The latter cells have many limitations, such as difficulties in utilizing the infra-red region of the solar spectrum, and instability for long-term uses. CdTe has a bulk band gap of 1.45 eV (Li et al., 2010; Madelung, 2004) with conduction and valance band energies at −4.3 and −5.7 eV vs. vacuum respectively (Kniprath et al., 2009). It also has an extinction coefficient of $4.4 \times 10^4\ M^{-1}\ cm^{-1}$ at 370 nm (Lan et al., 2009). These properties make it is QDs a good sensitizer, capable of effectively injecting electrons into TiO_2 NPs (band gap: 3.4 eV) (Li et al., 2010). In addition, when its' energy band gap is tuned close to the maximum of the solar spectrum, it allows an effective injection of photogenerated electrons from its conduction band (CB) to TiO_2 surface. There are many methods used to anchor QDs onto the large band gap metal oxides. Normally, these adsorption methods are: (1) *in situ* growth of QDs by either chemical bath deposition (CBD) technique (Xie et al., 2012; Prabakar et al., 2009; Lee et al., 2009), containing both the cationic and anionic precursors, or successive ionic layer adsorption and reaction deposition (SILAR) method (Mora-Seŕo, 2008; Ruhle et al., 2010; Zhang et al., 2012), and (2) *ex situ* growth as electrophoretic deposition (EPD) method (Smith et al., 2008; Salant et al., 2010), linker-assisted adsorption (LA) (Salant et al., 2010; Kongkanand et al., 2008; Pernik et al., 2011; Kamat, 2008), and direct adsorption (DA) technique (Gimḿenez et al., 2009; Guijarro and Lana-Villarreal, 2009; Pernik et al., 2011).

In this work, we prepared CdTe QDs of different sizes by organometallic pyrolysis method to be used as a sensitizer in QDSSCs. These colloidal QDs were adsorbed onto TiO_2 NPs by DA technique for different dipping times under ambient conditions. The effect of the CdTe QDs size on the QDSSCs characteristic parameters; short circuit current density (J_{sc}), open circuit voltage (V_{oc}), fill factor (FF), and efficiency (η) for energy conversion were studied. To the best of our knowledge, this is the first time that DA technique is used to deposit tuned band gap CdTe QDs onto TiO_2 NPs to assemble QDSSCs. Also, the photocurrent response of the assembled cells to ON–OFF cycles of the illumination was studied.

2. Experiment

2.1. Preparation of CdTe quantum dots

Colloidal CdTe nanocrystals were synthesized by organometallic pyrolysis method as described previously by Talapin et al. (2001) with little modification. The synthesis was carried out as follows: 2 g of dodecylamine (DDA) were dissolved in 7 mL of tri-*n*-octylphosphine (TOP) at 50 °C in a 50 mL two-neck flask with a reflux condenser attached. Subsequently, 0.11 mL (1.47 mmol) of dimethylcadmium and 0.128 g (1 mmol) of tellurium powder dissolved in TOP were added under stirring, and the temperature was slowly increased to 180 °C. After 30 min, the temperature was raised to 200 °C, then Te: TOP organometallic complex reacts slowly with Cd-precursor's to form CdTe nanoclusters. A sample was drown once the color of the solution change into orange indicating the formation of CdTe QDs. The reaction mixture heated up further to let the particles grow. The different sizes have been obtained at different reaction time intervals (30, 40, 60, and 80 min) and labeled (a–d). The samples were separated using centrifuge followed by surface treatment according to the method of Choi et al. (2006). Each sample of CdTe QDs was washed several times with methanol to remove excess ligands, then TOP/TOPO or TOPO/DDA ligands on the surface of CdTe QDs were replaced by refluxing the CdTe QDs in pyridine (20 mL) under 1 atm of N_2 for 24 h. The QDs were precipitated with toluene at room temperature.

2.2. Preparation of solar cell electrodes

The TiO_2 colloidal paste was prepared by the method of Syrrokostas et al. (2009). Three grams of commercial TiO_2 nanopowder (20 nm) (Degussa P-25 Titanium dioxide consists of 80% anatase and 20% rutile) was ground in a porcelain mortar and mixed with a small amount of distilled water (1 mL) containing acetyl acetone (10% v/v) to create the paste. Acetyl acetone was used as a dispersing agent, since it prevents coagulation of TiO_2 nanoparticles and affects the porosity of the film. The paste was diluted further by slow addition of distilled water (4 mL) under continued grinding. The addition of water controls the viscosity and the final concentration of the paste. Finally, a few drops of a detergent (Triton X-100) were added to facilitate the spreading of the paste on the substrate, since this substance has the ability to reduce surface tension, resulting in even spreading and reducing the formation of cracks. The TiO_2 paste was deposited on a conducting glass substrate of SnO_2: F with sheet resistance of 7 Ω/sq and >80% transmittance in the visible region, using a simple

doctor blade technique. This was followed by annealing at 450 °C for 30 min and the final thickness was 8 μm after the solvent evaporation. Then the TiO_2 films were dipped into a colloidal solution of pre-synthesized CdTe QDs to form working electrodes. The counter electrodes were prepared by coating another FTO substrate sheet with a resistance of 7 Ω/sq with Pt.

2.3. Assembly of QDSSC

The Pt counter electrode and CdTe QDs sensitized TiO_2 electrode were assembled as a sandwich type cell using clamps. Both electrodes were sealed using a hot-melt polymer sheet (solaronix, SX1170-25PF) of 25 μm thickness in order to avoid evaporation of the electrolyte. Finally, Iodide electrolyte solution was prepared by dissolving 0.127 g of 0.05 M Iodine (I_2) in 10 mL of water-free ethylene glycol, then adding 0.83 g of 0.5 M potassium iodide (KI). The electrolyte was inserted in the cell with a syringe, filling the space between the two electrodes.

2.4. Measurements

The absorption spectra of the CdTe QDs (before and after adsorption on TiO_2 electrodes) were recorded using a UV–Visible spectrophotometer (JASCO V-670). In addition, the sizes of the QDs were measured by high resolution transmission electron microscope (HRTEM) (JEOL JEM-2100 operated at 200 KV and equipped with Gatan CCD higher resolution camera). The current density–voltage (J–V) characteristics were recorded (with a Keithley 2400 voltage source/ammeter using GreenMountain IV-Sat 3.1 software), with the CdTe QDSSCs subjected to the irradiation of a solar simulator (ABET technologies, Sun 2000 Solar Simulators, USA) operating at 100 mW/cm^2 (AM1.5G). A Leybold certified silicon reference solar cell (Model: 57863) were used to calibrate the incident solar illumination. A J–V characteristic curve of all sizes of CdTe QDSSC were studied. All experiments were carried out under ambient conditions.

3. Results and discussion

3.1. Characterization of the CdTe QDs

The average particle size of all prepared CdTe QDs were estimated using HRTEM. Which ranged from 2.12 ± 0.13 nm to 2.53 ± 0.08 nm. Fig. 1a shows TEM micrographs of CdTe QDs sample d, while Fig. 1b and c shows HRTEM and histogram of particle size distribution for the same sample.

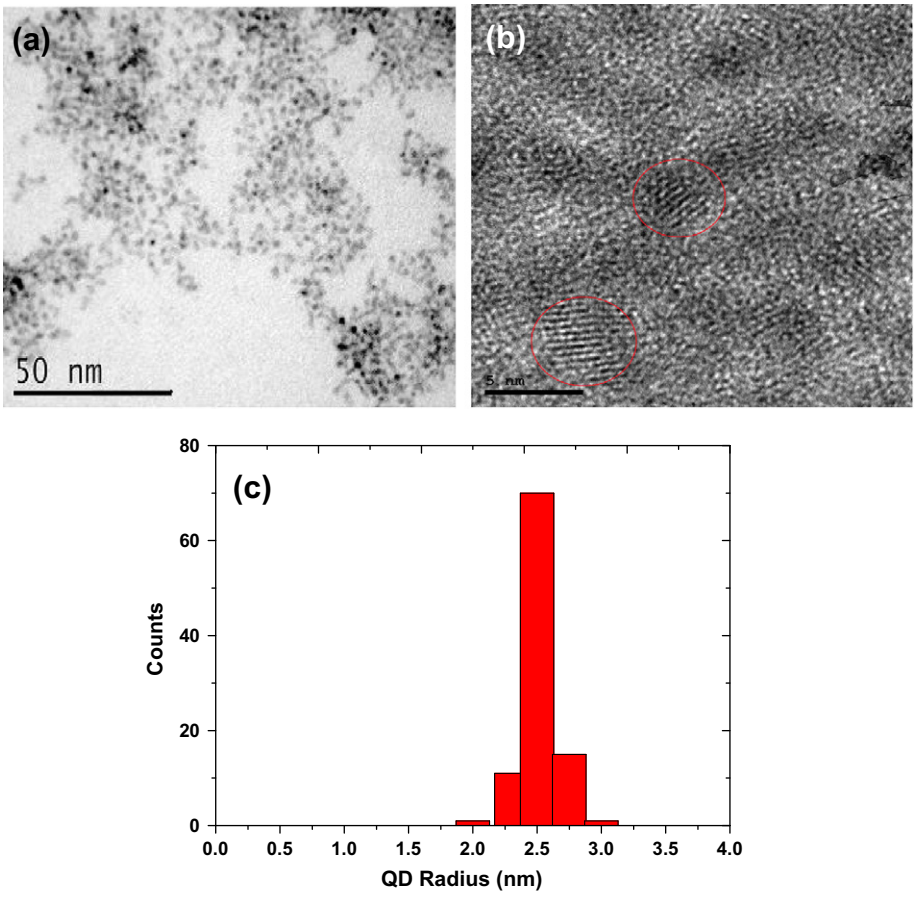

Fig. 1. (a) TEM micrograph for sample d, (b) HRTEM of CdTe QDs for sample d, and (c) Histogram of particle size distribution for CdTe QDs (sample d).

The UV–Visible absorption spectra of the samples (a–d) in colloidal solution are shown in Fig. 2. The excitonic absorption edges of these samples a–d are at: 533, 567, 575, and 602 nm respectively. The red shifts of the absorption to longer wavelengths with increasing particle size are due to the varying quantum confinement effect. The corresponding QDs radii were calculated using the effective mass approximation (EMA) model given by Yum et al. (2007), Brus (1986), Thambidurai et al. (2009) and Sathyamoorthy et al. (2010):

$$E_{g(\mathrm{Nano})}(R) = E_{g(\mathrm{Bulk})} + \frac{h^2}{8R^2}\left[\frac{1}{m_e} + \frac{1}{m_h}\right] - \frac{1.8e^2}{4\pi\varepsilon\varepsilon_0 R} \quad (1)$$

where $E_{g(\mathrm{Bulk})}$ (=1.475 eV) (Madelung, 2004) is the bulk CdTe crystal band gap value, $E_{g(\mathrm{Nano})}$ *is the nanocrystal band gap value,* R is the radius of CdTe QDs, h is Planck's constant, m_e (=0.11 m_0) (Trindade et al., 2001) and m_h (=0.35 m_0) (Trindade et al., 2001) are CdTe electron and hole effective masses respectively, and m_0 is electron mass, ε_0 is the permittivity of vacuum and ε (=7.1) is the relative dielectric constant for CdTe (Madelung, 2004). The calculated values are given as: 2.10, 2.27, 2.32 and 2.47 nm for samples a to d respectively. These values are in good agreement with those measured by HRTEM.

3.2. Characterization of CdTe QDs sensitized TiO_2 electrodes (the working electrode)

To ensure, that the adsorption of CdTe QDs onto the TiO_2 electrode takes place, EDX was performed for sample c of CdTe QDs adsorbed on TiO_2 electrode. The results are shown in Fig. 3 where the peaks of Cd and Te, as well as Ti are indicated.

The absorption spectra for each of the working electrodes of the four CdTe QDs sizes (a–d) dipped for four times (3, 6, 24, and 50 h) were measured. The UV–Visible absorption spectra for sample c (of radius 2.32 nm) sensitized TiO_2 electrode are given in Fig. 4. All other CdTe QDs onto TiO_2 electrode shows similar behavior. In all

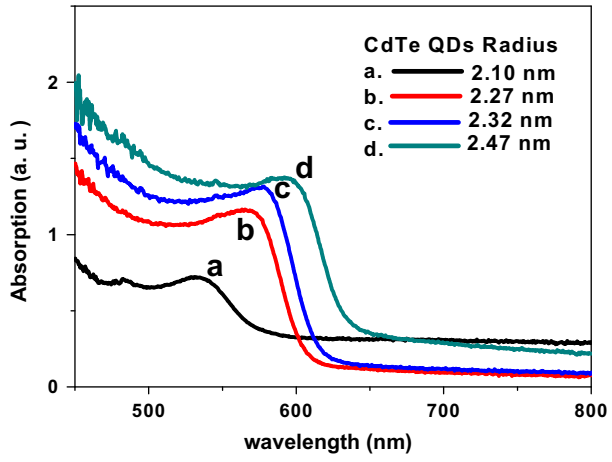

Fig. 2. UV–Visible absorption spectra for CdTe QDs samples (a–d).

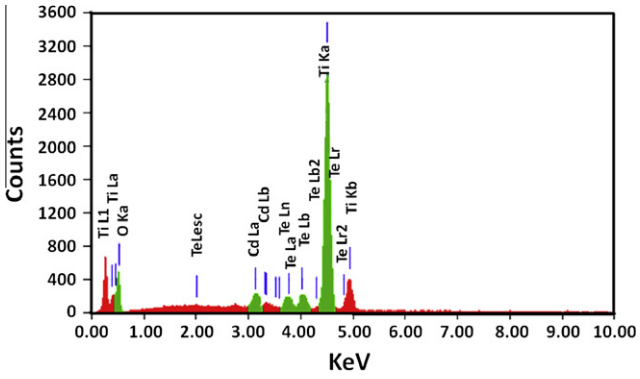

Fig. 3. EDX of sample c CdTe QDs adsorbed onto TiO_2 film.

cases, it is observed that the absorption spectra shifts toward the visible region with increasing the deposition time up to 24 h. Longer deposition time does no show appreciable difference from the 24 h deposition. However, the 50 h deposition time was used for determination of J–V characteristic curves.

3.3. Characterization of CdTe QDSSC

The J–V characteristics curves of the assembled CdTe QDSSCs where the TiO_2 photoelectrodes were dipped for 50 h in colloids of different sizes of CdTe QDs (a–d) are shown in Fig. 5. For solar illumination of 100 mW/cm^2.

It is clearly seen that as CdTe QDs size decreases, the values of J_{sc} increase and consequently η also increases. These results can be explained in term of the energetic alignments of CdTe QDs and those of TiO_2 NPs. The third term in Eq. (1) represents the coulomb energy which is generally very small quantity compared with the kinetic energy (second term), hence it can ignored (Franceschetti and Zunger, 1997; Mall et al., 2010; Kurian et al., 2007; Nandakumar et al., 2002). The energy change in the conduction band minimum (CBM) (lowest unoccupied molecular orbital (LUMO) levels) (Mall et al., 2010; Blackburn et al., 2005; Carlson et al., 2008; Sapra and Sarma, 2004), ΔE_{CBM} ($=\frac{h^2}{8m_eR^2}$). While the energy change in the valance band maximum (VBM) (highest occupied molecular orbital (HOMO) levels) (Mall et al., 2010; Blackburn et al., 2005; Carlson et al., 2008; Sapra and Sarma, 2004), ΔE_{VBM} ($=-\frac{h^2}{8m_hR^2}$). Since m_e is much smaller than m_h, the variation in ΔE_{CBM} is much more than that of ΔE_{VBM}. The calculated values of ΔE_{CBM} are: 0.78, 0.66, 0.64, and 0.56 eV, and of ΔE_{VBM} are: −0.24, −0.21, −0.20, and −0.18 eV for CdTe QDs (a–d) respectively. The value of the CB of bulk CdTe as deduced from the electron affinity (Mall et al., 2010; Movchan et al., 1999; Al-Ani et al., 2007) is −4.3 eV, which is close to the CB of TiO_2 at −4.3 eV vs. vacuum (Kniprath et al., 2009). The valance band (VB) for bulk CdTe is −5.7 eV vs. vacuum (Kniprath et al., 2009), which is well below the VB of the redox potential of I^-/I_3^- (=−4.94 eV vs. vacuum) (Yu et al., 2006). Fig. 6 shows the energetic alignments diagram of CdTe QDs

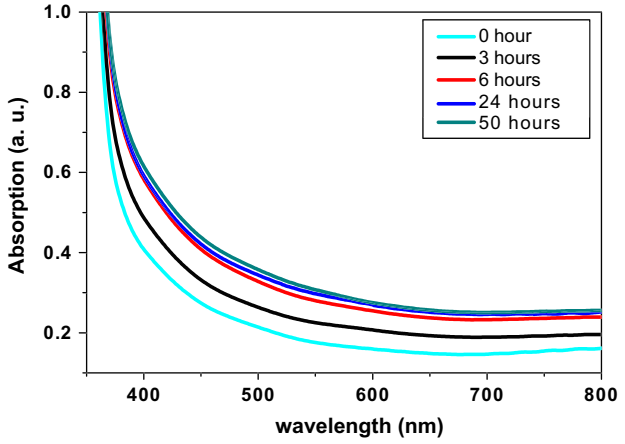

Fig. 4. UV–Visible absorption spectra of CdTe QDs (sample c: radius = 2.32 nm) deposited on TiO_2 NPs at 0, 3, 6, 24, and 50 h dipping time.

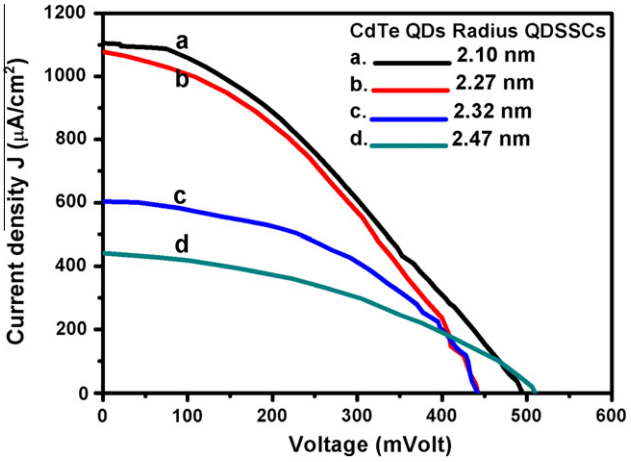

Fig. 5. *J–V* characteristic curve of CdTe QDSSCs for solar illumination of 100 mW/cm^2.

adsorbed onto the TiO_2 NPs surface as calculated from the above discussed variations ΔE_{CBM} and ΔE_{VBM}. It is to be observed that as the size of QDs decreases, the CB shifts closer to vacuum level, which causes an increase in the driving force. Consequently the electrons' injections to TiO_2 become faster, leading to an increase of the J_{sc}, and finally enhance η. Furthermore, we assume as the size of the QD decrease the whole surface area of the sensitizer increase and the number of QD per unit area of TiO_2 support increase, resulting in the harvest of more incident solar light and hence increasing J_{sc} and η. Similar results were obtained by Kongkanand et al. (2008). In their work they used CdSe QDs to sensitize TiO_2 NPs and nanotubes. They tuned the photo electrochemical response and photo conversion efficiency via size control of CdSe QDs, and reported that the maximum power-conversion efficiency was for 3 nm diameter (543 nm absorption edge) in close agreement with our results of CdTe QDs (533 nm absorption edge). In contrast of our result, Rolf Kniprath et al. (2009) concluded that CdTe QDSSC do not show any photocurrent at wavelengths in the absorption range of 450–650 nm, They attributed this behavior to the oxidation of surface states of Te (using thiol group in their preparation), which prevents charge transfer from the photo excited CdTe QDs to the TiO_2 NPs electrode.

The variations ΔE_{VBM} of CdTe QDs are approximately the same for all sizes ($\Delta E_{VBM} \sim -0.2$ eV), which is lower than that of CdTe bulk, and the regeneration of CdTe QDs by the redox couple in the electrolyte would be energetically favored. The values of the V_{oc} vary within about 67 mV for the QD sizes used (from 442 ± 10 mV to 507 ± 10 mV). We believe this variation may be due to possible change in the cell temperature during the measurement; however such variation will be the subject for future investigation. Furthermore, V_{oc} is only dictated by the CB level of TiO_2 NPs and the VB of the electrolyte (Kongkanand et al., 2008). Table 1 summarizes the characteristic parameters for the different sizes of CdTe QDSSCs.

The values of FF of the assembled cells comprised of CdTe QDs/TiO_2 photo electrode varies between 0.35 and 0.47, as seen in Table 1. the value of η is largest (0.19%) for the smallest size of CdTe QDs.

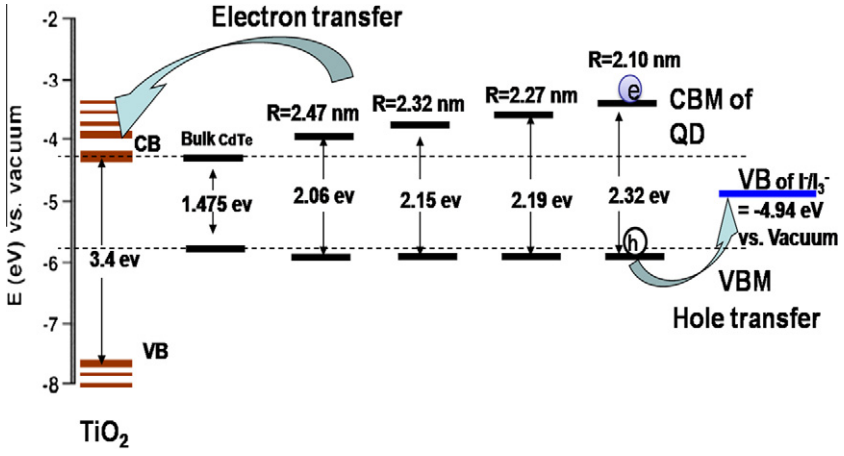

Fig. 6. Summary of energy diagram showing the alignment of the VBM and CBM of CdTe quantum dot to the TiO_2 valence and conduction bands (all data vs. vacuum).

Table 1
J–V characteristics parameters (J_{sc}, V_{oc}, FF and η) of CdTe QDSSCs for different QDs sizes, at dipping time = 50 h, under 1 sun illumination.

QDs size (nm) By EMA	QD energy Band gap (eV)	V_{oc} (±10 mV)	J_{sc} (μA/cm^2)	FF	Efficiency η (%)
2.10	2.30	495	1105	0.35	0.190
2.27	2.18	442	1087	0.38	0.181
2.32	2.14	440	603	0.47	0.125
2.47	2.06	507	441	0.40	0.091

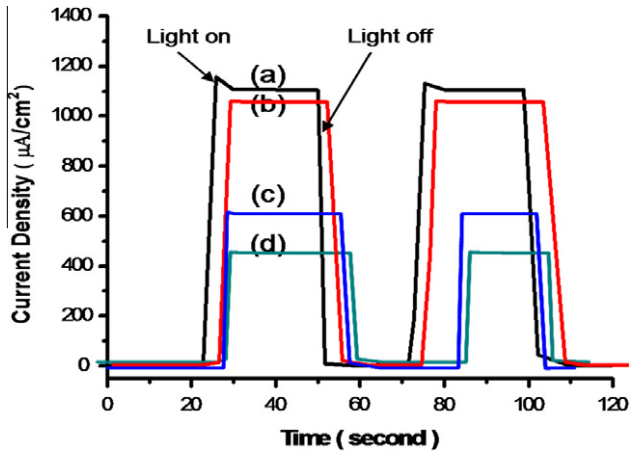

Fig. 7. Photocurrent response of CdTe QDSSCs to ON–OFF cycles to one sun illumination.

The photocurrent response to ON–OFF cycles to one sun illumination of samples a–d of CdTe QDSSCs for different QD sizes is presented in Fig. 7, where it is observed that the photocurrent generation was steady during ON–OFF cycles of the illumination, and it was maximum for the smallest CdTe QD size (2.10 nm). Also showing the prompt generation of anodic current.

4. Conclusions

CdTe QDs of different sizes were synthesized using the organometallic pyrolysis method and applied as sensitizers for QDSSCs by the DA technique onto TiO_2 NPs electrode. The open circuit voltages (V_{oc}) varies slightly with the size of the CdTe QDs, however it is only dictated by the CB level of TiO_2 NPs and the VB of the electrolyte. The values of J_{sc} and η increase as the QDs size decreases, since the LUMO of CdTe is shifted to more positive potential values with respect to that of TiO_2 NPs. The maximum values of J_{sc} (1105 μA/cm^2) and η (0.190%) were obtained for the smallest CdTe QDs size (2.10 nm). The photocurrent response of CdTe QDSSCs to ON–OFF cycles under one sun illumination shows prompt generation of anodic current.

Acknowledgements

The authors wish to thank Taif University for the financial support. Quantum Optics Research Group (QORG) at Taif University is also thanked for their assistance during this work. Prof. S. Negm and Prof. H. Talaat acknowledges generous support from the Egyptian STDF (ID 377).

References

Al-Ani, S.K.J., Ba-Yashoot, A.K., Makadsi, M.N., AI-Shabaty, A.M., 2007. Photovoltaic properties of n-$(ZnS)_X(CdTe)_{1-X}$/p-Si. Turk. J. Phys. 31, 259–264.

Bang, J.H., Kamat, P.V., 2009. Quantum dot sensitized solar cells. A tale of two semiconductor nanocrystals: CdSe and CdTe. ACS Nano 3, 1467–1476.

Blackburn, J.L., Selmarten, D.C., Ellingson, R.J., Jones, M., Micic, O., Nozik, A.J., 2005. Electron and hole transfer from indium phosphide quantum dots. J. Phys. Chem. B 109, 2625–2631.

Brus, L., 1986. Electronic wave functions in semiconductor clusters: experiment and theory. J. Phys. Chem. 90, 2555–2560.

Carlson, B., Leschkies, K., Aydil, E.S., Zhu, X.-Y., 2008. Valence band alignment at cadmium selenide quantum dot and Zinc Oxide(1010) interfaces. J. Phys. Chem. C 112, 8419–8423.

Choi, S.-H., Song, H., Park, I.K., Yum, J.-H., Kim, S.-S., Lee, S., Sung, Y.-E., 2006. Synthesis of size-controlled CdSe quantum dots and characterization of CdSe-conjugated polymer blends for hybrid solar cells. J. Photochem. Photobiol., A 179, 135–141.

Emin, S., Singh, S.P., Han, L., Satoh, N., Islam, A., 2011. Colloidal quantum dot solar cells. Sol. Energy 85, 1264–1282.

Fan, S.-Q., Kim, D., Kim, J.-J., Jung, D.W., Kang, S.O., Ko, J., 2009. Highly efficient CdSe quantum-dot-sensitized TiO_2 photoelectrodes for solar cell applications. Electron. Commun. 11, 1337–1339.

Franceschetti, A., Zunger, A., 1997. Direct pseudopotential calculation of exiton coulomb and exchange energies in semiconductor quantum dots. Phys. Rev. Lett. 78, 915–918.

Gimńenez, S., Mora-Seŕo, I.a., Macor, L., Guijarro, N., Lana-Villarreal, T., Ǵomez, R., Diguna, L.J., Shen, Q., Toyoda, T., Bisquert, J., 2009. Improving the performance of colloidal quantum-dot-sensitized solar cells. Nanotechnology 20, 295204.

Guijarro, N., Lana-Villarreal, T., Mora-Seró, I., Bisquert, J., Gómez, R., 2009. CdSe quantum dot-sensitized TiO_2 electrodes: effect of quantum dot coverage and mode of attachment. J. Phys. Chem. C 113, 4208–4214.

Hyun, B.-R., Zhong, Y.-W., Bartnik, A.C., Sun, L., Abrun, H.D., Wise, F.W., Goodreau, J.D., Matthews, J.R., Leslie, T.M., Borrelli, N.F., 2008. Electron injection from colloidal PbS quantum dots into titanium dioxide nanoparticles. ACS Nano 2, 2206–2212.

Kamat, P.V., 2007. Meeting the clean energy demand: nanostructure architectures for solar energy conversion. J. Phys. Chem. C 111, 2834–2860.

Kamat, P.V., 2008. Quantum dot solar cells. Semiconductor nanocrystals as light harvesters. J. Phys. Chem. C 112, 18737–18753.

Kim, J., Choi, H., Nahm, C., Moon, J., Kim, C., Nam, S., Jung, D.-R., Park, B., 2011. The effect of a blocking layer on the photovoltaic performance in CdS quantum-dot-sensitized solar cells. J. Power Sources 196, 10526–10531.

Kitada, S., Kikuchi, E., Ohnob, A., Aramakib, S., Maenosono, S., 2009. Effect of diamine treatment on the conversion efficiency of PbSe

colloidal quantum dot solar cells. Solid State Commun. 149, 1853–1855.

Kniprath, R., Rabe, J.P., McLeskey Jr., J.T., Wang, D., Kirstein, S., 2009. Hybrid photovoltaic cells with II–VI quantum dot sensitizers fabricated by layer-by-layer deposition of water-soluble components. Thin Solid Films 518, 295–298.

Kongkanand, A., Tvrdy, K., Takechi, K., Kuno, M., Kamat, P.V., 2008. Quantum dot solar cells. Tuning photoresponse through size and shape control of CdSe–TiO_2 architecture. J. Am. Chem. Soc. 130, 4007–4015.

Kurian, P.A., Vijayan, C., Sathiyamoorthy, K., Sandeep, C.S.S., Philip, R., 2007. Excitonic transitions and off-resonant optical limiting in CdS quantum dots stabilized in a synthetic glue matrix. Nanoscale Res. Lett. 2, 561–568.

Lan, G.-Y., Yang, Z., Lin, Y.-W., Lin, Z.-H., Liao, H.-Y., Chang, H.-T., 2009. A simple strategy for improving the energy conversion of multilayered CdTe quantum dot-sensitized solar cells. J. Mater. Chem. 19, 2349–2355.

Lee, W., Min, S.K., Dhas, V., Ogale, S.B., Han, S.-H., 2009. Chemical bath deposition of CdS quantum dots on vertically aligned ZnO nanorods for quantum dots-sensitized solar cells. Electron. Commun. 11, 103–106.

Li, Y.-S., Jiang, F.-L., Xiao, Q., Li, R., Li, K., Zhang, M.-F., Zhang, A.-Q., Sun, S.-F., Liu, Y., 2010. Enhanced photocatalytic activities of TiO_2 nanocomposites doped with water-soluble mercapto-capped CdTe quantum dots. Appl. Catal. B: Environ. 101, 118–129.

Li, Y., Pang, A., Zheng, X., Wei, M., 2011. CdS quantum-dot-sensitized Zn_2SnO_4 solar cell. Electrochim. Acta 56, 4902–4906.

Lin, M.-C., Lee, M.-W., 2011. $Cu_{2-x}S$ quantum dot-sensitized solar cells. Electron. Commun. 13, 1376–1378.

Madelung, O., 2004. Semiconductors: Data Handbook, third ed. Springer-Verlag, Berlin.

Mall, M., Kumar, P., Chand, S., Kumar, L., 2010. Influence of ZnS quantum dots on optical and photovoltaic properties of poly(3-hexylthiophene). Chem. Phys. Lett. 495, 236–240.

McCandless, B.E., Dobson, K.D., 2004. Processing options for CdTe thin film solar cells. Sol. Energy 77, 839–856.

Mora-Seŕo, I.a., Gimenez, Sixto, Moehl, T., Fabregat-Santiago, F., Lana-Villareal, T., Ǵomez, R., Bisquert, J., 2008. Factors determining the photovoltaic performance of a CdSe quantum dot sensitized solar cell: the role of the linker molecule and of the counter electrode. Nanotechnology 19, 424007.

Movchan, S., Sizov, F., Tetyorkin, V., 1999. Photosensitive heterostructures CdTe–PbTe prepared by hot-wall technique. Semicond. Phys., Quantum Electron Optoelectron 2, 84–87.

Nandakumar, P., Vijayan, C., Murti, Y.V.G.S., 2002. Optical absorption and photoluminescence studies on CdS quantum dots in Nafion. J. Appl. Phys. 91, 1509–1514.

Nozik, A.J., 2008. Multiple exciton generation in semiconductor quantum dots. Chem. Phys. Lett. 457, 3–11.

Pernik, D.R., Tvrdy, K., Radich, J.G., Kamat, P.V., 2011. Tracking the adsorption and electron injection rates of CdSe quantum dots on TiO_2: linked versus direct attachment. J. Phys. Chem. C 115, 13511–13519.

Prabakar, K., Seo, H., Son, M., Kim, H., 2009. CdS quantum dots sensitized TiO_2 photoelectrodes. Mater. Chem. Phys. 117, 26–28.

Ruhle, S., Shalom, M., Zaban, A., 2010. Quantum-dot-sensitized solar cells. Chem. Phys. Chem. 11, 2290–2304.

Salant, A., Shalom, M., Hod, I., Faust, A., Zaban, A., Banin, U., 2010. Quantum dot sensitized solar cells with improved efficiency prepared using electrophoretic deposition. ACS Nano 4, 5962–5968.

Sapra, S., Sarma, D.D., 2004. Evolution of the electronic structure with size in II–VI semiconductor nanocrystals. Phys. Rev. B 69, 125304.

Sathyamoorthy, R., Sudhagar, P., Kumar, R.S., Sathyadevan, T.M., 2010. Low temperature synthesis of thiol-functionalized CdTe nanoclusters with different tellurium contents. Cryst. Res. Technol. 45, 99–103.

Smith, N.J., Emmett, K.J., Rosenthal, S.J., 2008. Photovoltaic cells fabricated by electrophoretic deposition of CdSe nanocrystals. Appl. Phys. Lett. 93, 043504.

Syrrokostas, G., Giannouli, M., Yianoulis, P., 2009. Effects of paste storage on the properties of nanostructured thin films for the development of dye-sensitized solar cells. Renew. Energy 34, 1759–1764.

Talapin, D.V., Haubold, S., Rogach, A.L., Kornowski, A., Haase, M., Weller, H., 2001. A novel organometallic synthesis of highly luminescent CdTe nanocrystals. J. Phys. Chem. B 105, 2260–2263.

Thambidurai, M., Murugan, N., Muthukumarasamy, N., Vasantha, S., Balasundaraprabhu, R., Agilan, S., 2009. Preparation and characterization of nanocrystalline CdS thin films. Chalcogenide Lett. 6, 171–179.

Timp, B.A., Zhu, X.-Y., 2010. Electronic energy alignment at the PbSe quantum dots/ZnO(1010) interface. Surf. Sci. 604, 1335–1341.

Trindade, T., O'Brien, P., Pickett, N.L., 2001. Nanocrystalline semiconductors: synthesis, properties, and perspectives. Chem. Mater. 13, 3843–3858.

Tubtimtae, A., Wu, K.-L., Tung, H.-Y., Lee, M.-W., Wang, G.J., 2010. Ag_2S quantum dot-sensitized solar cells. Electron. Commun. 12, 1158–1160.

Tubtimtae, A., Lee, M.-W., Wang, G.-J., 2011. Ag_2Se quantum-dot sensitized solar cells for full solar spectrum light harvesting. J. Power Sources 196, 6603–6608.

Tvrdy, K., Kamat, P.V., 2009. Substrate driven photochemistry of CdSe quantum dot films: charge injection and irreversible transformations on oxide surfaces. J. Phys. Chem. A 113, 3765–3772.

Tvrdy, K., Frantsuzov, P.A., Kamat, P.V., 2011. Photoinduced electron transfer from semiconductor quantum dots to metal oxide nanoparticles. PNAS 108, 29–34.

Wang, X., Zhu, H., Xu, Y., Wang, H., Tao, Y., Hark, S., Xiao, X., Li, Q., 2010. Aligned ZnO/CdTe core shell nanocable arrays on indium tin oxide: synthesis and photoelectrochemical properties. ACS Nano 4, 3302–3308.

Wijayanthaa, K.G.U., Petera, L.M., Otley, L.C., 2004. Fabrication of CdS quantum dot sensitized solar cells via a pressing route. Sol. Energy Mater. Sol. Cells 83, 363–369.

Wu, X., 2004. High-efficiency polycrystalline CdTe thin-film solar cells. Sol. Energy 77, 803–814.

Xie, Y., Yoo, S.H., Chen, C., Cho, S.O., 2012. Ag_2S quantum dots-sensitized TiO_2 nanotube array photoelectrodes. Mater. Sci. Eng.: B 177, 106–111.

Yang, Z., Chang, H.-T., 2010. CdHgTe and CdTe quantum dot solar cells displaying an energy conversion efficiency exceeding 2%. Sol. Energy Mater. Sol. Cells 94, 2046–2051.

Yong Kim, J., Chung, I.J., Chul Kim, Y., Yu, J.-W., 2004. Nanocrystal-conjugated polymer photovoltaic devices. J. Korean Phys. Soc. 45, 231–234.

Yu, P., Zhu, K., Norman, A.G., Ferrere, S., Frank, A.J., Nozik, A.J., 2006. Nanocrystalline TiO_2 solar cells sensitized with InAs quantum dots. J. Phys. Chem. B 110, 25451–25454.

Yu, X.-Y., Lei, B.-X., Kuang, D.-B., Su, C.-Y., 2011. Highly efficient CdTe/CdS quantum dot sensitized solar cells fabricated by a one-step linker assisted chemical bath deposition. Chem. Sci. 2, 1396–1400.

Yum, J.-H., Choi, S.-H., Kim, S.-S., Kim, D.-Y., Sung, Y.-E., 2007. CdSe quantum dots sensitized TiO_2 electrodes for photovoltaic cells. J. Korean Phys. Soc. 10, 257–261.

Zhang, Y., Zhu, J., Yu, X., Wei, J., Hu, L., Dai, S., 2012. The optical and electrochemical properties of CdS/CdSe co-sensitized TiO_2 solar cells prepared by successive ionic layer adsorption and reaction processes. Sol. Energy 86, 964–971.

Zhao, F., Tang, G., Zhang, J., Lin, Y., 2012. Improved performance of CdSe quantum dot-sensitized TiO_2 thin film by surface treatment with $TiCl_4$. Electrochim. Acta 62, 396–401.

Zhou, J., Song, B., Zhao, G., Dong, W., Han, G., 2012. TiO_2 nanorod arrays sensitized with CdSe quantum dots for solar cell applications: effects of rod geometry on photoelectrochemical performance. Appl. Phys. A 107, 321–331.